Tomographic reconstruction of quantum correlations in excited Bose-Einstein condensates

Anders S. Mouritzen*† and Klaus Mølmer‡

QUANTOP, Danish National Research Foundation Center for Quantum Optics,
Department of Physics and Astronomy, University of Aarhus, DK-8000 Århus C, Denmark

(Dated: 2nd February 2008)

We propose to use quantum tomography to characterize the state of a perturbed Bose-Einstein condensate. We assume knowledge of the number of particles in the zero-wave number mode and of density distributions in space at different times, and we treat the condensate in the Bogoliubov approximation. For states that can be treated with the Gross-Pitaevskii equation, we find that the reconstructed density operator gives excellent predictions of the second moments of the atomic creation- and annihilation operators, including the one-body density matrix. Additional inclusion of the momentum distribution at one point of time enables somewhat reliable predictions to be made for the second moments for mixed states, making it possible to distinguish between coherent and thermal perturbations of the condensate. Finally, we find that with observation of the zero-wave number mode's anomalous second moment, $\langle \hat{a}_0 \hat{a}_0 + \hat{a}_0^\dagger \hat{a}_0^\dagger \rangle$, the reconstructed density operator gives reliable predictions of the second moments of locally amplitude squeezed states.

PACS numbers: 03.65.Wj 42.50.Gy

I. INTRODUCTION

Bose-Einstein condensates offer countless demonstrations of macroscopic quantum effects [1], [2]. Recently, there has been growing interest in the use of condensates as quantum optical components and as atom laser beam sources. The effective use of very many of these applications requires knowledge of certain aspects of the condensate's quantum state, and several articles have dealt with theoretical calculations of the states obtained by various perturbations of a condensate.

We present here a method by which experimental data can be used to estimate characteristics of the system's quantum state. For this purpose we generalize the application of the Jaynes principle of maximum entropy (MAXENT) [3] for quantum state tomography, as proposed in [4] and applied to single atoms in [5] and [6], to the dynamics of a condensate described in the Bogoliubov approximation. We assume that the fraction of particles in the zero-wave number mode and the position distributions at different times after preparation of the system have been measured. It is important to note that we are not claiming that the MAXENT density operator is an approximation to the true many-body operator of the quantum state; indeed this would surely require more than just density measurements (one-body operators). Instead, we seek to correctly predict the second moments of the atomic creation- and annihilation operators $\hat{\psi}(x)$ and $\hat{\psi}^\dagger(x)$. Because these second moments of the ladder operators will be discussed extensively below, we shall call second moments of the form $\langle \hat{\psi}^\dagger(x)\hat{\psi}^\dagger(x') \rangle$

and $\langle \hat{\psi}(x)\hat{\psi}(x') \rangle$ anomalous second moments, while second moments of the form $\langle \hat{\psi}^\dagger(x)\hat{\psi}(x') \rangle$ will be referred to as normal second moments.

As an example of applying the method, three types of quantum mechanically very different states will be studied. First, we study states characterized by a single Gross-Pitaevskii wave function with small deviations from the constant value attained by the ground state homogeneous condensate. Then secondly, we apply our method to an incoherently exited system, modeled by the addition of a localized thermal component to the homogeneous condensate. Finally, as a third case, we study the method's fidelity for a system with a localized amplitude squeezed atomic field.

Our paper is organized as follows. In section II we give a brief introduction to the central ideas behind tomography and a description of the procedure for reconstructing the density operator of a quantum system by use of Jaynes principle of maximum entropy. In section III we specify our assumptions about the condensate, and we introduce the Bogoliubov approximation and the general para-unitary transformation procedure. In section IV we will combine the MAXENT and Bogoliubov theories. In section V, we apply the machinery to the three different trial states. In section VI we discuss the applicability of the method and we finally conclude the paper in section VII.

II. QUANTUM STATE TOMOGRAPHY

A. Tomography

Can you find all the peaks of a mountain landscape or draw a map of a city just by seeing its skylines from all compass directions? Of course not: obstacles may block your line of vision, no matter from which angle you look,

---

*Comments should be directed to this person
†Electronic address: asm@phys.au.dk
‡Electronic address: moelmer@phys.au.dk

making it impossible to determine the layout. The central idea behind tomography is the, somewhat surprising, fact that if you had performed absorption measurements from all angles, instead of looking at shadows, you could indeed have found every detail of the area.

Finding its first application in medicine, tomography techniques have been used extensively in this field since the 1970's. Here, tomography is used to reconstruct 3-D pictures from data recorded using X-rays or NMR.

With regard to quantum systems, tomography can be used to reconstruct the density matrix of the system. For quantum harmonic oscillator systems this reconstruction can be done exactly by measuring the quadrature distributions for all quadrature angles; for example measuring the density distribution in space for all points of time during one period of oscillation. The techniques for this include the inverse Radon transformation [7], [8] and the more reliable technique of pattern functions [9]. The analogy to the absorption measurements mentioned earlier is apparent if one considers the quadrature distributions as marginal distributions of the system's Wigner function.

Buzěk and Drobný have shown that a good approximation to the density matrix for the one-particle harmonic oscillator can be achieved using the MAXENT principle with the observations of just a few quadrature distributions and the mean oscillator excitation number [4]. Skovsen et al. recently used MAXENT tomography to reconstruct the one-body density matrix of free particles from experimental data [6].

In this paper we will extend the scope of MAXENT quantum tomography by using it to approximately reconstruct the second moments of the ladder operators, including the one-body density matrix, of a many-particle system: a condensate treated in the Bogoliubov approximation.

B. MAXENT principle for reconstruction of density operators

The method we use to estimate the quantum state of our system at hand is by finding the MAXENT density operator as suggested by Jaynes [3]. The goal of the method is to find a density operator that exactly reproduces the knowledge one has about the system while making as few assumptions as possible about degrees of freedom one has no knowledge about. A proposal for this is the maximum entropy density operator $\hat{\rho}_{ME}$ chosen for having maximal von Neumann entropy $S = -Tr(\hat{\rho} \ln \hat{\rho})$. We make this more rigorous in the following way [20]:

Let a set of observables $\{\hat{G}_\nu\}, (\nu \in 1, 2, \ldots, n)$ be associated with a quantum system prepared in an unknown state $\hat{\rho}$. We imagine an ensemble of these quantum systems wherein there are no correlations between the subsystems of the ensemble, and we assume to have measured the ensemble expectation values $\{\bar{G}_\nu\}$ of the observables $\{\hat{G}_\nu\}$.

Unless the set of observables $\{\hat{G}_\nu\}$ constitutes the *quorum* (a complete set of observables) there will in general be many density operators $\hat{\rho}_{\{\hat{G}\}}$ that satisfy the normalization condition $Tr(\hat{\rho}_{\{\hat{G}\}}) = 1$ and predict the measured values:

$$Tr(\hat{\rho}_{\{\hat{G}\}} \hat{G}_\nu) = \bar{G}_\nu, \quad \nu \in \{1, 2, \ldots, n\}. \qquad (1)$$

The MAXENT principle says that the most unbiased guess for the density operator approximating $\hat{\rho}$ and fulfilling these conditions is the one with maximal von Neumann entropy:

$$S(\hat{\rho}_{ME}) = \max\left[S(\hat{\rho}_{\{\hat{G}\}}); \forall \hat{\rho}_{\{\hat{G}\}}\right], \qquad (2)$$

$$S(\hat{\rho}) = -Tr(\hat{\rho} \ln \hat{\rho}). \qquad (3)$$

As shown by Jaynes [3] this implies a density operator of the form:

$$\hat{\rho}_{ME} = \frac{1}{Z_{\{\hat{G}\}}} \exp\left(-\sum_{\nu=1}^{n} \lambda_\nu \hat{G}_\nu\right) \qquad (4)$$

with the generalized partition function:

$$Z_{\{\hat{G}\}} = Tr\left[\exp\left(-\sum_{\nu=1}^{n} \lambda_\nu \hat{G}_\nu\right)\right] \qquad (5)$$

and with the $\{\lambda_\nu\}$ being a set of Lagrange multipliers chosen so that ρ_{ME} in Eq. (4) fulfills the conditions Eqs. (1). Using these λ_ν's we have the explicit form of the MAXENT density operator Eq. (4).

A technical difficulty arises because, in all but the most trivial circumstances, it is not feasible to analytically invert the conditions Eqs. (1) given Eq. (4) to obtain the set $\{\lambda_\nu\}$. For implementation it is more convenient, and we shall indeed use this procedure, to minimize the norm of the differences between measured values and values predicted by $\hat{\rho}_{ME}$ with respect to $\{\lambda_\nu\}$:

$$\begin{pmatrix} Tr(\hat{\rho}_{ME}(\{\lambda_\nu\})\hat{G}_1) - \bar{G}_1 \\ \vdots \\ Tr(\hat{\rho}_{ME}(\{\lambda_\nu\})\hat{G}_n) - \bar{G}_n \end{pmatrix} \qquad (6)$$

Here, we have given the same weight to all components of the vector of errors. One may wish to modify this if, for instance, some observations are made with a much better precision than others.

III. DESCRIPTION OF THE CONDENSATE

A. Bogoliubov Hamiltonian

Let us consider a 3-dimensional cold gas of atoms having mass m, occupying a volume V, and dominated by

s-wave collisions where $U(r, r') = U_0 \delta(r - r')$ is the inter-particle potential. Such a gas is well represented by the Hamiltonian:

$$H_{full} = \sum_k \varepsilon_k \hat{a}_k^\dagger \hat{a}_k + \frac{g}{2} \sum_{k,k',q} \hat{a}_{k+q}^\dagger \hat{a}_{k'-q}^\dagger \hat{a}_{k'} \hat{a}_k \quad (7)$$

where $\varepsilon_k = \frac{\hbar^2 k^2}{2m}$ is the free-particle energy and $g = \frac{U_0}{V}$ is the coupling constant. The operators $\hat{a}_k$ and $\hat{a}_k^\dagger$ are the usual boson ladder operators annihilating and creating a particle with wave vector k, and having the commutation relations:

$$[\hat{a}_k, \hat{a}_{k'}^\dagger] = \delta_{k,k'} \quad (8)$$
$$[\hat{a}_k, \hat{a}_{k'}] = 0. \quad (9)$$

A Hamiltonian similar to Eq. (7) applies in one and two spatial dimensions with suitable redefinitions of g, depending on the confinement of the remaining coordinates [10], [11]. For simplicity, only one spatial dimension will be used in this paper. The wave vectors k are then merely scalars, and will in the following be referred to as wave numbers.

Due to the complicated dynamics of the Hamiltonian Eq. (7), it is often necessary to use an approximate Hamiltonian to make analytical calculations possible. We will employ the so-called Bogoliubov approximation, which is valid when the vast majority of the particles are in the zero wave number mode [12]:

$$\langle \hat{a}_0^\dagger \hat{a}_0 \rangle \gg \sum_{k \neq 0} \langle \hat{a}_k^\dagger \hat{a}_k \rangle. \quad (10)$$

Having this condition fulfilled, it is a good approximation to approximate the Hamiltonian Eq. (7) by [21]:

$$\hat{H} = \frac{1}{2} \sum_{k \neq 0} \left((\varepsilon_k + gN_{tot})(\hat{a}_k^\dagger \hat{a}_k + \hat{a}_k \hat{a}_k^\dagger) + \right.$$
$$\left. + gN_{tot}(\hat{a}_k \hat{a}_{-k} + \hat{a}_{-k}^\dagger \hat{a}_k^\dagger) \right) \quad (11)$$

and N_{tot} is the total number of particles in the gas. This operator is bilinear in the ladder operators, and can be diagonalized by a change of basis. We will do this by using elementary linear algebra.

B. Discretization of position and momentum

We will now specify some useful technical details of our treatment. We consider an odd number ($N > 1$) of evenly spaced points in 1-D coordinate space, symmetrically distributed around (and including) the origin, on an interval of length $L = N \Delta x$.

$$x_n = n \Delta x, \qquad n = -M, -M+1, \ldots, M \quad (12)$$

where $M = \frac{N-1}{2}$. We assume that the spatial atomic density is measured on this grid, i.e., our observations

will be of the form $\langle \hat{\psi}^\dagger(x_n, t) \hat{\psi}(x_n, t) \rangle$. Due to the form of the Hamiltonian Eq. (11), it is convenient to introduce the discrete wave numbers corresponding to the spatial discretization above.

$$k_q = q \Delta k, \qquad \Delta k = \frac{2\pi}{L}, \quad (13)$$

where q can assume the same values as n above.

The usual discrete Fourier transform from coordinate space ($\hat{\psi}(x_n)$ and $\hat{\psi}^\dagger(x_n)$) to wave number space ($\hat{a}(k_q)$ and $\hat{a}^\dagger(k_q)$) reads:

$$\hat{a}(k_q) = \frac{1}{\sqrt{N}} \sum_{n=-M}^{M} \hat{\psi}(x_n) \exp(ik_q x_n) \quad (14)$$

$$\hat{a}^\dagger(k_q) = \frac{1}{\sqrt{N}} \sum_{n=-M}^{M} \hat{\psi}^\dagger(x_n) \exp(-ik_q x_n). \quad (15)$$

All the ladder operators in coordinate space can be arranged in a $2N \times 1$ column vector:

$$\boldsymbol{\psi} = \begin{pmatrix} \hat{\psi}(x_{-M}) \\ \vdots \\ \hat{\psi}(x_M) \\ \hat{\psi}^\dagger(x_{-M}) \\ \vdots \\ \hat{\psi}^\dagger(x_M) \end{pmatrix}, \quad (16)$$

and correspondingly:

$$\boldsymbol{\psi}^\dagger = \left(\hat{\psi}^\dagger(x_{-M}), \ldots, \hat{\psi}^\dagger(x_M), \hat{\psi}(x_{-M}), \ldots, \hat{\psi}(x_M) \right). \quad (17)$$

In this paper, we shall denote vectors of this type by bold letters. Similarly, we can construct the column vector $\boldsymbol{a}$ from the operators in wave number space $\hat{a}(k_q)$ and $\hat{a}^\dagger(k_q)$:

$$\boldsymbol{a} = \begin{pmatrix} \hat{a}(k_{-M}) \\ \vdots \\ \hat{a}(k_M) \\ \hat{a}^\dagger(k_{-M}) \\ \vdots \\ \hat{a}^\dagger(k_M) \end{pmatrix}, \quad (18)$$

Using these vectors, we can write the Fourier transformation Eqs. (14)–(15) as a matrix multiplication by a $2N \times 2N$ matrix:

$$\boldsymbol{a} = \mathscr{A} \cdot \boldsymbol{\psi}, \quad \text{whereby} \quad \boldsymbol{a}^\dagger = \boldsymbol{\psi}^\dagger \cdot \mathscr{A}^\dagger. \quad (19)$$

Here, and in the following, we shall use script letters to denote matrices of dimension $2N \times 2N$.

The matrix $\mathscr{A}$ has the following form:

$$\mathscr{A} = \begin{pmatrix} F & 0 \\ 0 & F^* \end{pmatrix} \quad (20)$$

and F is the usual $N \times N$ discrete Fourier transformation matrix, whose q'th row is:

$$F(q, :) = \frac{1}{\sqrt{N}} [\exp(ik_q x_{-M}), \ldots, \exp(ik_q x_M)] \quad (21)$$

from which Eqs. (14)–(15) are easily recovered.

It is straightforward to see that the operators $\hat{a}(k_q)$ and $\hat{\psi}(x_n)$ obey similar commutation relations Eqs. (8)-(9). In this paper we shall exclusively deal with transformations to new sets of operators that conserve this property.

C. Diagonalization of the Bogoliubov Hamiltonian

Using the notation developed in the preceding section, we can write the Bogoliubov Hamiltonian Eq. (11) in a compact form:

$$\hat{H} = \boldsymbol{a}^\dagger \mathscr{H} \boldsymbol{a}. \quad (22)$$

As shown in e.g. [13], this Hamiltonian can be diagonalized to the matrix $\mathscr{E}$ by transforming to new boson operators:

$$\boldsymbol{b} = \mathscr{B} \boldsymbol{a} \quad (23)$$

$$\begin{aligned} \hat{H} &= \boldsymbol{a}^\dagger \mathscr{H} \boldsymbol{a} \\ &= \boldsymbol{a}^\dagger \mathscr{B}^\dagger (\mathscr{B}^\dagger)^{-1} \mathscr{H} \mathscr{B}^{-1} \mathscr{B} \boldsymbol{a} \\ &= \boldsymbol{b}^\dagger (\mathscr{B}^\dagger)^{-1} \mathscr{H} \mathscr{B}^{-1} \boldsymbol{b} \\ &= \boldsymbol{b}^\dagger \mathscr{E} \boldsymbol{b}, \end{aligned} \quad (24)$$

$$\mathscr{E} = (\mathscr{B}^\dagger)^{-1} \mathscr{H} \mathscr{B}^{-1}. \quad (25)$$

The matrix $\mathscr{H}$ only has elements different from zero in the two diagonals $\mathscr{H}(k_q, k_q)$ and $\mathscr{H}(k_q, k_{-q})$, giving the matrix an "X-structure". In addition, all elements are real. Therefore the matrix $\mathscr{B}^{-1}$ that diagonalizes $\mathscr{H}$ also only has elements different from zero with these indices, and can be chosen real. The upper-left to lower-right diagonal elements are denoted $u(k_q)$, while the upper-right to lower-left diagonal elements are denoted $v(k_q)$. The elements can be found in e.g. [14]:

$$u(k_q) = \begin{cases} 1 & \text{for } q = 0 \\ \sqrt{\frac{q^2/4 + \gamma/2}{\epsilon(q)/E_0} + \frac{1}{2}} & \text{for } q \neq 0 \end{cases}$$

$$v(k_q) = \begin{cases} 0 & \text{for } q = 0 \\ -\sqrt{\frac{q^2/4 + \gamma/2}{\epsilon(q)/E_0} - \frac{1}{2}} & \text{for } q \neq 0. \end{cases}$$

The diagonalized form $\mathscr{E}$ has elements $\epsilon(k_q)$:

$$\epsilon(k_q) = E_0 \sqrt{\gamma q^2 + q^4/4} \quad (26)$$

where $E_0 = \frac{(2\pi\hbar)^2}{mL^2}$, $\gamma = \frac{gN_{tot}}{E_0}$, and gN_{tot} has the same meaning as in Eq. (11).

By diagonalizing the Hamiltonian we have found a basis of non-interacting modes with a simple time evolution:

$$\hat{b}_q(t) = \hat{b}_q(0) \exp(-i\epsilon(q)t/\hbar).$$

By defining the para-identity matrix $\hat{\mathscr{I}}$, which will play an important role in the next section:

$$\hat{\mathscr{I}} = diag(\underbrace{1, \ldots, 1}_{N}, \underbrace{-1, \ldots, -1}_{N}) \quad (27)$$

we can write the vector of operators $\boldsymbol{b}$ at time t as:

$$\boldsymbol{b}(t) = \exp(-i\hat{\mathscr{I}}\mathscr{E}t/\hbar)\boldsymbol{b}(0) = \mathscr{U}(t)\boldsymbol{b}(0). \quad (28)$$

The changes of basis can be summarized like this:

$$\begin{aligned} \boldsymbol{\psi}(t) &= \mathscr{A}^{-1} \boldsymbol{a}(t) \\ &= \mathscr{A}^{-1} \mathscr{B}^{-1} \boldsymbol{b}(t) \\ &= \mathscr{A}^{-1} \mathscr{B}^{-1} \mathscr{U}(t) \boldsymbol{b}(0), \end{aligned} \quad (29)$$

whereby we can find the time evolution of the $\hat{\psi}(x_n, t)$ and $\hat{\psi}^\dagger(x_n, t)$:

$$\boldsymbol{\psi}(t) = \mathscr{A}^{-1} \mathscr{B}^{-1} \mathscr{U}(t) \mathscr{B} \mathscr{A} \boldsymbol{\psi}(0). \quad (30)$$

D. General para-unitary diagonalization

All the vectors of operators Eq. (16), Eq. (18) and Eq. (23) are examples of a vector of general boson ladder operators:

$$\boldsymbol{\alpha} = \begin{pmatrix} \hat{\alpha}_{-M} \\ \vdots \\ \hat{\alpha}_M \\ \hat{\alpha}_{-M}^\dagger \\ \vdots \\ \hat{\alpha}_M^\dagger \end{pmatrix}, \quad (31)$$

fulfilling the commutation relations:

$$[\hat{\alpha}_q, \hat{\alpha}_{q'}^\dagger] = \delta_{q,q'} \quad (32)$$
$$[\hat{\alpha}_q, \hat{\alpha}_{q'}] = 0 \quad (33)$$

Both the Fourier transformation Eq. (19) and the Bogoliubov transformation Eq. (23) are examples of changes of basis, known as para-unitary transformations, which conserve the Boson commutation relations between the operators. All the transformations to new sets of operators in this paper conserve this property. In our present treatment, there are two main reasons for making these transformations. Firstly, the measurements we have performed on the system are in the coordinate space and wave number space at different times, but the operators corresponding to these measurements have complicated time evolutions. Working instead in the $\boldsymbol{b}$-basis

Eq. (28) the time evolution is simple, and the exponent in Eq. (4) can be easily calculated. Secondly, to perform the traces in Eq. (6), it is convenient to shift to a basis where the density operator is diagonal, and this can be done by a para-unitary transformation. We recall that there are $2N$ ladder operators, regardless of basis (f.x. the set $\{\hat{\psi}(x_n)\}$ and $\{\hat{\psi}^\dagger(x_n)\}$), which will make the transformation matrices $2N \times 2N$.

The commutation relations demand that in a transformation from one set of boson operators to another:

$$\boldsymbol{\beta} = \mathscr{T}\boldsymbol{\alpha} \qquad (34)$$

the $2N \times 2N$ matrix $\mathscr{T}$ must be para-unitary, i.e. satisfy the condition [22]:

$$\hat{\mathscr{I}} = \mathscr{T}\hat{\mathscr{I}}\mathscr{T}^\dagger \qquad (35)$$

with the diagonal matrix $\hat{\mathscr{I}}$ defined in Eq. (27) [23]. From the definition it is seen that the product of two para-unitary matrices is again para-unitary.

The matrices we will diagonalize in this paper will all be hermitian, positive definite and have the structure [24]:

$$\mathscr{X} = \begin{pmatrix} P & Q \\ Q^* & P^* \end{pmatrix}. \qquad (36)$$

Let $\hat{X}$ be a hermitian operator in the $\boldsymbol{\alpha}$ basis with coefficient matrix $\mathscr{X}$. Such a hermitian matrix $\mathscr{X}$ can be diagonalized by the para-unitary matrix $\mathscr{T}$ to a new set of operators $\{\beta_n\}$ and $\{\beta_n^\dagger\}$:

$$\begin{aligned} \hat{X} &= \boldsymbol{\alpha}^\dagger \mathscr{X} \boldsymbol{\alpha} \qquad (37) \\ &= \boldsymbol{\alpha}^\dagger \mathscr{T}^\dagger (\mathscr{T}^\dagger)^{-1} \mathscr{X} \mathscr{T}^{-1} \mathscr{T} \boldsymbol{\alpha} \\ &= \boldsymbol{\beta}^\dagger (\mathscr{T}^\dagger)^{-1} \mathscr{X} \mathscr{T}^{-1} \boldsymbol{\beta} \\ &= \boldsymbol{\beta}^\dagger \mathscr{L} \boldsymbol{\beta}. \qquad (38) \end{aligned}$$

Because $\mathscr{X}$ is positive definite the para-eigenvalues $\mathscr{L}_{i,i}$ will also be positive by Sylvester's law of inertia. The matrix $\mathscr{T}$ can be chosen to have the structure:

$$\mathscr{T} = \begin{pmatrix} U & V^* \\ V & U^* \end{pmatrix} \qquad (39)$$

giving $\mathscr{L}$ the form:

$$\mathscr{L} = diag(\mathscr{L}_{1,1}, \mathscr{L}_{2,2}, \ldots, \mathscr{L}_{N,N}, \mathscr{L}_{1,1}, \ldots, \mathscr{L}_{N,N}). \qquad (40)$$

This general procedure will become useful in the following section, where we will need to evaluate expectation values of the observed densities within a quantum state of the form Eq. (4), facilitated by a para-unitary diagonalization of the exponent $\sum_\nu \lambda_\nu \hat{G}_\nu$.

IV. USING MAXENT WITH THE BOGOLIUBOV APPROXIMATION

Now we are ready to use the MAXENT formalism on the condensate in the Bogoliubov approximation. As the set of observables $\{\hat{G}_\nu\}$ we use measurements of particle numbers at coordinate space points at different times t, and of the occupation of wave number modes at times t'. The times t can, but need not, be equal to the times t'

$$\begin{aligned} \{\hat{G}_\nu\} =\ & \{\hat{\psi}^\dagger(x_n,t)\hat{\psi}(x_n,t) + \hat{\psi}(x_n,t)\hat{\psi}^\dagger(x_n,t)\} \bigcup \\ & \{\hat{a}^\dagger(k_q,t')\hat{a}(k_q,t') + \hat{a}(k_q,t')\hat{a}^\dagger(k_q,t')\}. \quad (41) \end{aligned}$$

The reason for using this symmetrical form of the observables is that it leads to the favorable structure Eq. (36) of the matrix in the exponent of Eq. (4).

The task is now to put these observables into the MAXENT density operator Eq. (4) and perform traces like Eqs. (1). To do this we will use the same method as in section II to diagonalize the matrix in the exponent into a set of new, non-interacting quasi-particles.

Let $\mathscr{W}_n$ be the $2N \times 2N$ matrix with the following elements:

$$\mathscr{W}_n(r,s) = \begin{cases} 1 & \text{for } r = s = n + M + 1 \\ 1 & \text{for } r = s = n + N + M + 1 \\ 0 & \text{otherwise} \end{cases} \qquad (42)$$

so that (using Eq. (29) for the first part):

$$\hat{\psi}^\dagger(x_n,t)\hat{\psi}(x_n,t) + \hat{\psi}(x_n,t)\hat{\psi}^\dagger(x_n,t) = \boldsymbol{\psi}^\dagger(t)\mathscr{W}_n\boldsymbol{\psi}(t)$$

$$= \boldsymbol{b}^\dagger(0)\mathscr{U}^\dagger(t)\left(\mathscr{B}^{-1}\right)^\dagger \left(\mathscr{A}^{-1}\right)^\dagger \mathscr{W}_n \mathscr{A}^{-1}\mathscr{B}^{-1}\mathscr{U}(t)\boldsymbol{b}(0) \qquad (43)$$

$$\hat{a}^\dagger(k_q,t')\hat{a}(k_q,t') + \hat{a}(k_q,t')\hat{a}^\dagger(k_q,t') = \boldsymbol{a}^\dagger(t')\mathscr{W}_q\boldsymbol{a}(t')$$

$$= \boldsymbol{b}^\dagger(0)\mathscr{U}^\dagger(t')\left(\mathscr{B}^{-1}\right)^\dagger \mathscr{W}_q\mathscr{B}^{-1}\mathscr{U}(t')\boldsymbol{b}(0). \qquad (44)$$

The operator $\sum_\nu \lambda_\nu \hat{G}_\nu$, with $\hat{G}_\nu$ being operators of the form Eq. (43) and Eq. (44) is hence expressed in terms of the Bogoliubov eigenmode operators, and we can write the MAXENT density operator Eq. (4) in a compact form:

$$\hat{\rho}_{ME} = \frac{1}{Z}\exp\left(-\boldsymbol{b}^\dagger(0)\mathscr{P}\boldsymbol{b}(0)\right), \qquad (45)$$

where

$$\begin{aligned} \mathscr{P} =\ & \sum_t \sum_{n=-M}^{M} \lambda(n,t) \cdot \\ & \mathscr{U}^\dagger(t)\left(\mathscr{B}^{-1}\right)^\dagger \left(\mathscr{A}^{-1}\right)^\dagger \mathscr{W}_n \mathscr{A}^{-1}\mathscr{B}^{-1}\mathscr{U}(t) \\ & + \sum_{t'} \sum_{q=-M}^{M} \lambda(q,t') \cdot \\ & \mathscr{U}^\dagger(t')\left(\mathscr{B}^{-1}\right)^\dagger \mathscr{W}_q\mathscr{B}^{-1}\mathscr{U}(t'). \qquad (46) \end{aligned}$$

Since the structures of $\mathscr{U}(t)$, $\mathscr{A}$ and $\mathscr{B}$ are all like that of Eq. (39), and the structure of $\mathscr{W}_q$ is like that of Eq. (36), so is the structure of $\mathscr{P}$. We can therefore diagonalize it to a diagonal matrix $\mathscr{L}$ by a para-unitary change of basis to new Boson operators $\boldsymbol{c} = \mathscr{C}\boldsymbol{b}(0)$:

$$\boldsymbol{b}^{\dagger}(0)\mathscr{P}\boldsymbol{b}(0) = \boldsymbol{c}^{\dagger}\mathscr{L}\boldsymbol{c} \qquad (47)$$

$$= \sum_{j=1}^{N} \mathscr{L}_{j,j}\left(\hat{c}_{j}^{\dagger}\hat{c}_{j} + \hat{c}_{j}\hat{c}_{j}^{\dagger}\right). \qquad (48)$$

Remembering that the $\mathscr{L}_{j,j}$ are all positive, the partition function Eq. (5) becomes:

$$Z = Tr\left(\exp\left[-\sum_{j=1}^{N}\mathscr{L}_{j,j}\left(\hat{c}_{j}^{\dagger}\hat{c}_{j} + \hat{c}_{j}\hat{c}_{j}^{\dagger}\right)\right]\right)$$

$$= \prod_{j=1}^{N}\left(\frac{1}{\exp\left(\mathscr{L}_{jj}\right) - \exp\left(-\mathscr{L}_{jj}\right)}\right), \qquad (49)$$

and we can readily determine the corresponding set of expectation values:

$$\langle\hat{c}_{m}^{\dagger}\hat{c}_{n}\rangle = \frac{1}{Z}Tr\left(\hat{c}_{m}^{\dagger}\hat{c}_{n}\exp\left[\sum_{j=1}^{N}\mathscr{L}_{j,j}\left(\hat{c}_{j}^{\dagger}\hat{c}_{j} + \hat{c}_{j}\hat{c}_{j}^{\dagger}\right)\right]\right)$$

$$= -\frac{1}{2}\left(1 + \frac{\partial \ln Z}{\partial\mathscr{L}_{n,n}}\right)\delta_{m,n}$$

$$= \frac{1}{\exp(2\mathscr{L}_{n,n}) - 1}\delta_{m,n} \qquad \text{and} \qquad (50)$$

$$\langle\hat{c}_{m}\hat{c}_{n}\rangle = \langle\hat{c}_{m}^{\dagger}\hat{c}_{n}^{\dagger}\rangle = 0. \qquad (51)$$

Knowing these expectation values, it is easy to find the expectation values of all the second moments in any basis, for example:

$$\langle\boldsymbol{\psi}(t)\boldsymbol{\psi}^{\dagger}(t)\rangle =$$

$$\begin{pmatrix} \langle\hat{\psi}(x_{-M})\hat{\psi}^{\dagger}(x_{-M})\rangle & \cdots & \langle\hat{\psi}(x_{-M})\hat{\psi}(x_{-M})\rangle & \cdots \\ \vdots & \ddots & \vdots & \ddots \\ \langle\hat{\psi}^{\dagger}(x_{-M})\hat{\psi}^{\dagger}(x_{-M})\rangle & \cdots & \langle\hat{\psi}^{\dagger}(x_{-M})\hat{\psi}(x_{-M})\rangle & \cdots \\ \vdots & \ddots & \vdots & \ddots \end{pmatrix}$$

$$= \mathscr{A}^{-1}\langle\boldsymbol{a}(t)\boldsymbol{a}^{\dagger}(t)\rangle\left(\mathscr{A}^{-1}\right)^{\dagger}$$

$$= \left[\mathscr{C}\mathscr{U}^{-1}(t)\mathscr{B}\mathscr{A}\right]^{-1}\langle\boldsymbol{c}\boldsymbol{c}^{\dagger}\rangle \cdot$$

$$\left\{\left[\mathscr{C}\mathscr{U}^{-1}(t)\mathscr{B}\mathscr{A}\right]^{-1}\right\}^{\dagger}.$$

In passing, it is noted that the lower right $N \times N$ submatrix of the matrix $\langle\boldsymbol{\psi}(t)\boldsymbol{\psi}^{\dagger}(t)\rangle$ is the one-body density matrix.

As a final point we give a comment on the requirement of the positive definiteness of $\mathscr{P}$. It is clearly seen here that we must require the diagonal elements of $\mathscr{L}$ to be strictly positive for the geometrical series summed to find Eq. (49) to be convergent. Therefore, by Sylvester's law of inertia, $\mathscr{P}$ must also be positive definite. In addition, for this condition to be fulfilled, the number of observables in $\{\hat{G}_{\nu}\}$ must be at least as large as N. The reason for this is that in Eq. (46) the matrices $\mathscr{W}_{n}$ have dimensionality two in the $2N$ space, the dimensionality of course being conserved under the para-unitary changes of basis. So to span the $2N$ space, at least N observables of dimensionality two must be included. In the present paper, however, we will have many more observations than N, and linear dependencies between them are highly unlikely to reduce the dimensionality below $2N$.

V. TOMOGRAPHY ON THREE QUANTUM STATES

A. Initial excited states

The time evolution is given by Eq. (30). Since we are not attempting to reconstruct the full many-particle quantum state, but only the second moments of the ladder operators, it is hence sufficient to specify these at, for example, $t = 0$:

$$\langle\boldsymbol{\psi}(t)\boldsymbol{\psi}^{\dagger}(t)\rangle =$$
$$\mathscr{A}^{-1}\mathscr{B}^{-1}\mathscr{U}(t)\mathscr{B}\mathscr{A}\langle\boldsymbol{\psi}(0)\boldsymbol{\psi}^{\dagger}(0)\rangle \cdot$$
$$\left[\mathscr{A}^{-1}\mathscr{B}^{-1}\mathscr{U}(t)\mathscr{B}\mathscr{A}\right]^{\dagger}. \qquad (52)$$

To examine the reliability of the MAXENT technique, regarding reconstruction of the correct second moments of the ladder operators, we study three very different types of condensate quantum states with nearly the same density distribution at $t = 0$: namely a gaussian perturbation on top of a flat condensate.

1. **Coherent state** is a pure state of all the particles, representable as a product state with all the particles in the same state. We choose this to be a constant with a gaussian perturbation in coordinate space.

$$|State\,1\rangle = \left(\hat{\psi}_{g}^{\dagger}\right)^{N_{part}}|0\rangle, \quad \text{where} \qquad (53)$$

$$\hat{\psi}_{g}^{\dagger} = \sum_{x_{n}}\phi_{gauss}(x_{n})\hat{\psi}^{\dagger}(x_{n}) \qquad (54)$$

and ϕ_{gauss} is a constant plus a gaussian with standard deviation σ, centered at the origin: $\phi_{gauss} \propto \left\{1 + \eta\exp\left[-\frac{1}{2}\left(\frac{x_{n}}{\sigma}\right)^{2}\right]\right\}$. N_{part} is the total number of particles. We can envision this state formed in a uniform system with a negative potential dip, having $State\,1$ as its ground state. The spatial evolution of the state after abruptly turning off the potential at $t = 0$ is what is usually handled with

the Gross-Pitaevskii equation:

$$-i\hbar\frac{\partial\psi}{\partial t} = \left(-\frac{\hbar^2}{2m}\frac{\partial^2}{\partial x^2} + gN_{tot}|\psi|^2\right)\psi. \quad (55)$$

2. **Thermal perturbation** This state is a flat condensate with a thermal gaussian perturbation superposed hereupon. The gaussian perturbation is treated as originating from a thermal boson gas in a harmonic trap and we have assumed no initial correlations between the perturbation and the original flat condensate. Therefore the second moments for this state in coordinate space are simply the sum for the thermal gaussian and the flat condensate.

3. **Squeezed condensate** We get this state by applying an operator, similar to the squeezing operator known from squeezing of light, to a condensate with all N_{part} particles in the condensate mode:

$$|State\,3\rangle = \exp\left[z^*(\hat{\psi}_g)^2 - z(\hat{\psi}_g^\dagger)^2\right]\left(\hat{b}_0^\dagger\right)^{N_{part}}|0\rangle. \quad (56)$$

The most important difference between the two preceding states and this one is the magnitude of the anomalous second moments at $t = 0$. In $State\,1$ and 2 the anomalous second moments are all zero, where they in this state are comparable in magnitude with the normal second moments.

B. Results of tomography

We present here the results of using the MAXENT technique on the three states discussed in section V A. The main points of interest are not just whether a reliable reconstruction is attained, but also the amount of data needed for this. In all the results shown in this section we have used density distributions in coordinate space at four different times. In $State\,2$ we have furthermore used the momentum distribution at $t = 0$, and in $State\,3$ we have additionally included an observation of $\langle\hat{a}_0\hat{a}_0 + \hat{a}_0^\dagger\hat{a}_0^\dagger\rangle$.

We have used 10^5 particles in the flat part of the condensate at $t = 0$ and set $gN_{tot} = 0.1$. The population in the zero wave number modes is 99.5% in $State\,1$ and 3 and 96% in $State\,2$. For the calculations we have used a grid of $N = 25$ discrete points.

In Fig. 1 we show the density distributions in coordinate space of the three different states declared in section V A. We have intentionally chosen the initial distributions to be very similar. The perturbations give rise to density variations of a magnitude readily detected [15].

We now proceed to examine the true second moments of the ladder operators for the three states and those reconstructed using the MAXENT procedure. We will study these using surface plots of the absolute value of the second moments and of the absolute value of the difference between the true values of these moments and
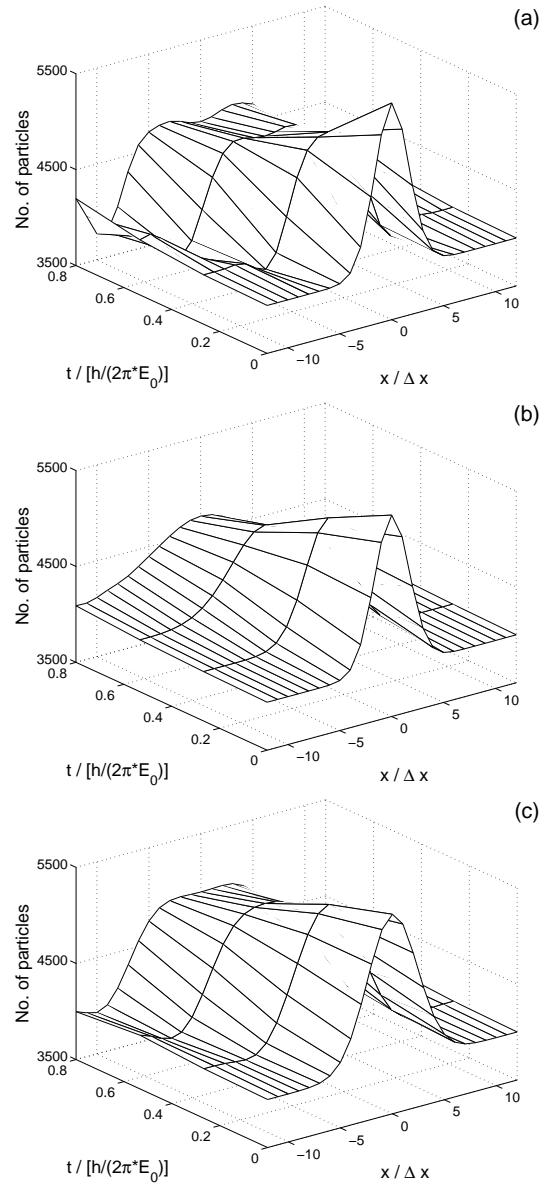

Figure 1: Density distributions in coordinate space at four different points of time for: (a) $State\,1$, (b) $State\,2$ and (c) $State\,3$. The data shown are those used in the calculations together with momentum distributions at $t = 0$ for $State\,2$ and 3, and one anomalous moment for $State\,3$.

those predicted by MAXENT for the state at $t = 0$. In this way, errors in both magnitude and phase of the matrix elements will be visible.

For $State\,1$, where we will see that the reconstruction is precise and only the normal second moments are non-zero at $t = 0$, we shall also display the phase-space Wigner function corresponding to these normal second moments. Apart from normalization, the normal second moments can be interpreted as the density matrix for any single atom in the system, and the phase space Wigner function $W(x_n, k_q)$ is a convenient representation of this. The cited works [4], [5], [6] all show the Wigner function of the

particle states, and much interest has been devoted to the fact that measurements of exclusively positive marginal distributions may be used to identify Wigner functions with domains of negative values [16], [17]. The connection between the Wigner function and the normal second moments is given in appendix B.

1. State 1

Treating first *State* 1, Fig. 2 presents the absolute value of the normal second moments as found from section V A. The reconstructed second moments are identical to the input values within roundoff errors, which amounts to an accumulated error of 10^{-4} on each matrix element, including phase. The same is true for the anomalous second moments, all having the true value zero at $t = 0$.
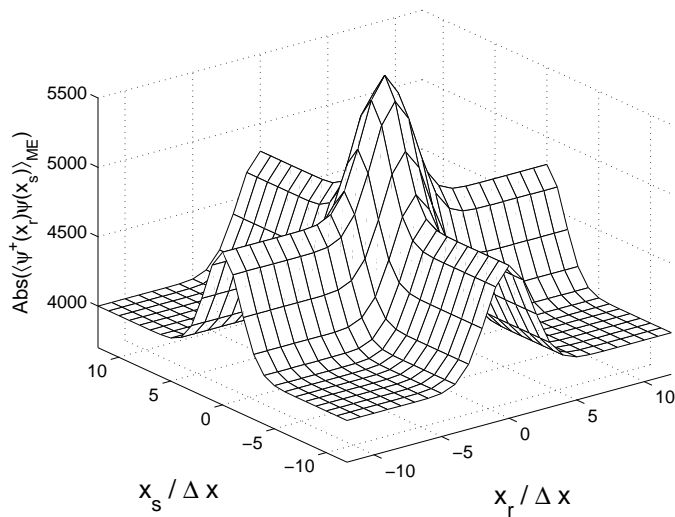
Figure 2: Absolute value of the reconstructed normal second moments $\langle \hat{\psi}^\dagger(x_r)\hat{\psi}(x_s) \rangle$ of *State* 1. The anomalous second moments are all zero (not shown). Both normal and anomalous moments are reconstructed to within machine precision, including complex phase, giving accumulated errors of magnitude 10^{-4} on each element. The data used for the reconstruction are four spatial density distributions. The true second moments are not shown, as they are practically identical to the reconstructed ones.

As a consequence, the Wigner function for *State* 1 is also perfectly reconstructed, and is presented in Fig. 3.

2. State 2

For *State* 2 the true and reconstructed normal second moments are shown in Fig. 4. Also shown in this figure is the absolute value of the difference between the true and reconstructed normal second moments. The errors are many orders of magnitude larger than for *State* 1.
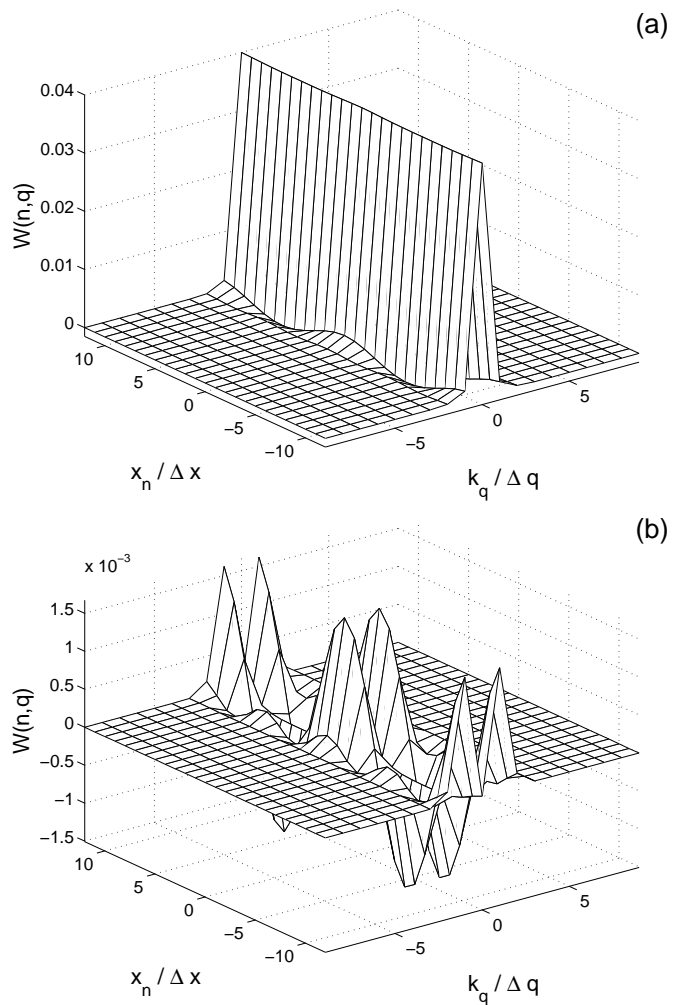

Figure 3: The upper graph (a) shows the Wigner function for the normal second moments of *State* 1, i.e. the one-body density matrix apart from normalization. In the lower graph (b) the elements W(n,0) are set equal to zero to more clearly reveal the finer structures and the negativities of the Wigner function.

In Fig. 5 we display the absolute value of the reconstructed anomalous second moments, that all have the true value zero at $t = 0$.

3. State 3

The absolute value of the true and reconstructed second moments are shown in Fig. 6 together with the absolute value of the difference between these.

In *State* 1 and 2, the true value of the anomalous second moments have all been equal to zero at $t = 0$. In contrast, for the squeezed state, the absolute value of these elements are comparable with the normal second moments. The absolute value of the true and reconstructed second anomalous moments are displayed in Fig. 7.
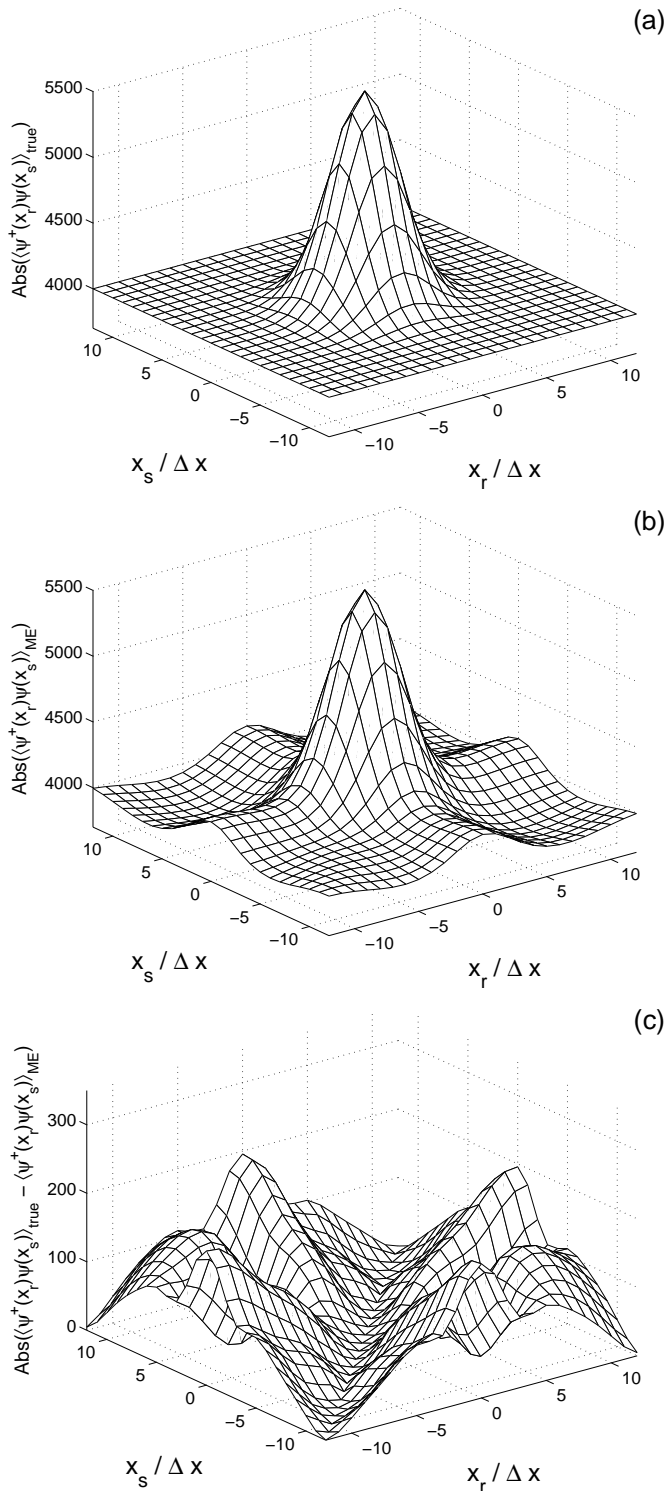
(a)

(b)

(c)

Figure 4: The first two graphs show the absolute value of (a) the true, and (b) the reconstructed normal second moments $\langle\hat\psi^\dagger(x_r)\hat\psi(x_s)\rangle$ for $State\,2$. The errors above the condensate are up to about 10% of the peak value. The bottom graph (c) shows the absolute value of the difference between true and reconstructed normal second moments. The data used in the reconstruction are four spatial density distributions and one momentum distribution.
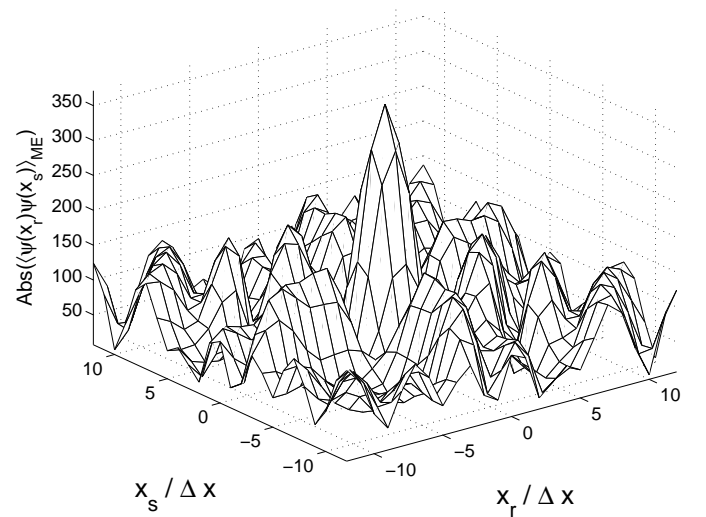

Figure 5: Absolute value of the reconstructed anomalous second moments $\langle\hat\psi(x_r)\hat\psi(x_s)\rangle$ for $State\,2$ at $t=0$. The true values are all zero at $t=0$. The magnitude of the errors is similar to the errors of the normal second moments for this state.

VI. DISCUSSION

Initially, a short comment on the choice of observables might be in order. If there were no constant background condensate the momentum distribution could in principle be found from the spatial distributions at late times. Having to deal with this background, however, one has to include the additional observables in the MAXENT density operator to exclude the possibility of the flat part of the condensate being an almost even distribution of particles with all allowed types of wave numbers whirling left and right, which would otherwise be preferred by the MAXENT formalism.

Indeed we find for $State\,1$ a very good reconstruction, the errors being of the same magnitude as computer roundoff errors, from using just measurements of the distribution in coordinate space at three times and the number of particles in the zero wave number mode $\langle\hat a^\dagger(0)\hat a(0)\rangle$. In addition to $State\,1$ in section V B, we also tried to reconstruct states of this type with more complicated initial distributions, but still describable by a simple Gross-Pitaevskii wave function. These included perturbations with two peaks and perturbations with one peak and one hole in the flat background. In all cases the reconstruction had the same precision as $State\,1$, indicating that the second moments, including the one-body density matrix, of states describable by a simple Gross-Pitaevskii equation can be completely reconstructed.

For $State\,2$, we found that a wave number distribution also had to be included as observable to get a somewhat reliable reconstruction of the second moments. It is reasonable that it is difficult to tell apart whether the moving particles belong to the perturbation on top of a
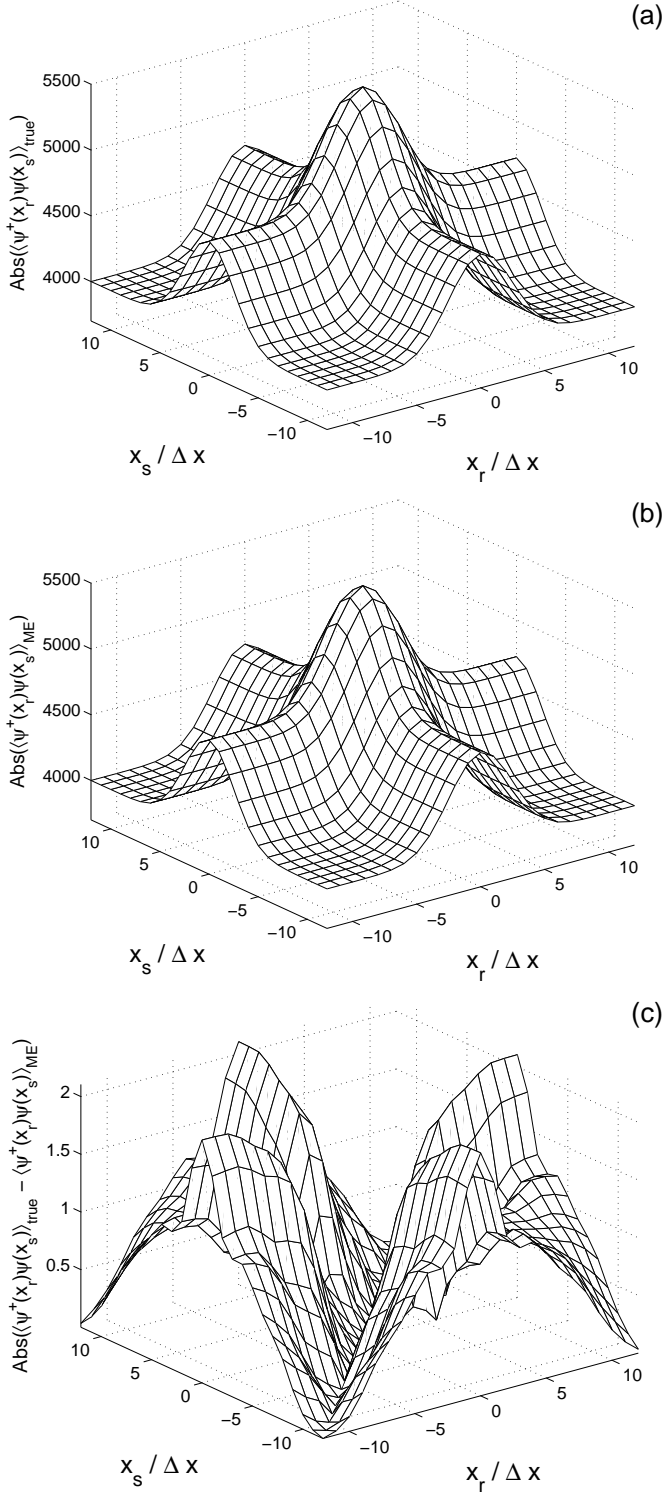
(a)

(a)

(b)

(b)

(c)

(c)

Figure 6: The first two graphs show the absolute value of (a) the true, and (b) the reconstructed normal second moments $\langle\hat{\psi}^\dagger(x_r)\hat{\psi}(x_s)\rangle$ of $State\,3$. The lowest graph (c) is the absolute value of the difference between the true and reconstructed second moments. The data used in the reconstruction are four spatial density distributions, one momentum distribution and $\langle\hat{a}_0\hat{a}_0 + \hat{a}_0^\dagger\hat{a}_0^\dagger\rangle$.
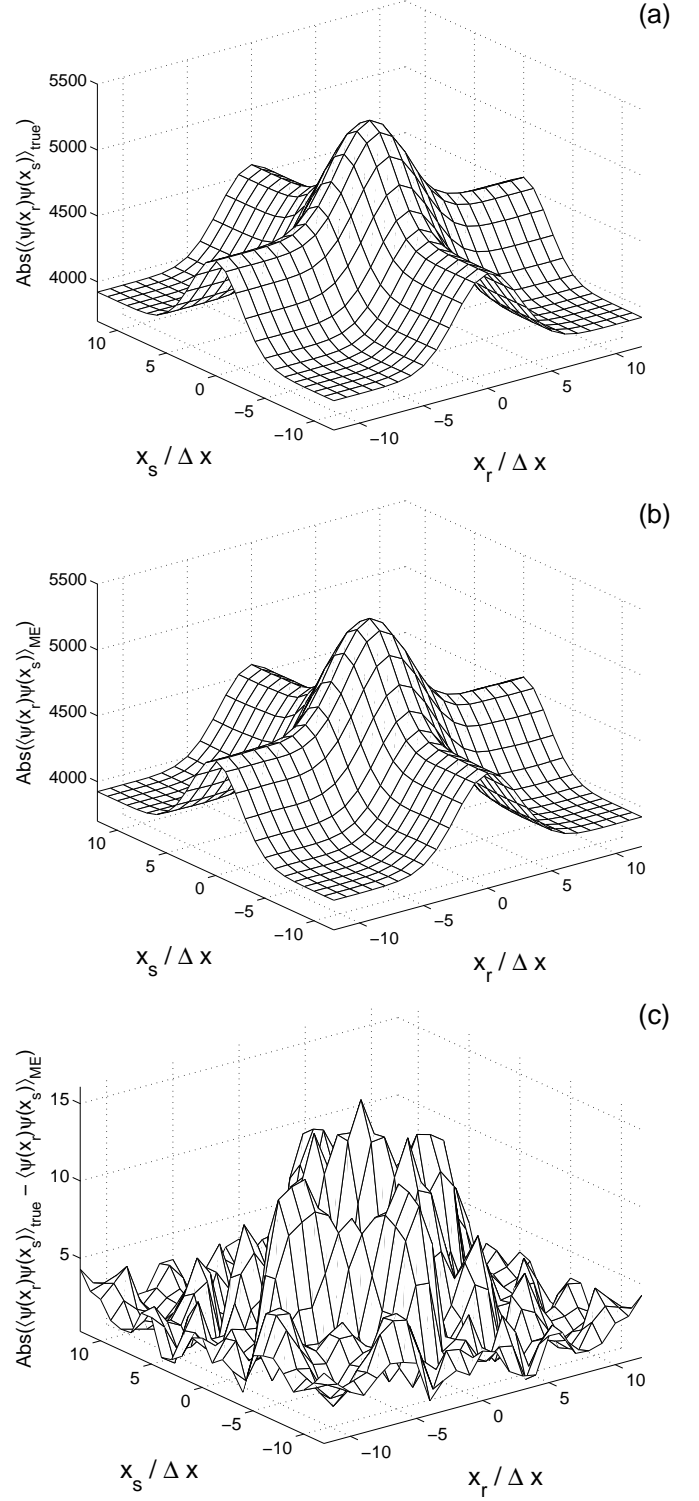
Figure 7: The first two graphs show the absolute value of (a) the true, and (b) the reconstructed anomalous second moments $\langle\hat{\psi}(x_r)\hat{\psi}(x_s)\rangle$ of $State\,3$. The lowest graph (c) is the absolute value of the difference between the true and reconstructed second moments. The data used in the reconstruction are four spatial density distributions, one momentum distribution and $\langle\hat{a}_0\hat{a}_0 + \hat{a}_0^\dagger\hat{a}_0^\dagger\rangle$.

flat condensate or to some collective motion of the whole, for example similar to *State* 1. Including the momentum distribution remedied this problem somewhat, but errors still persist (see Fig. 4). Subtracting the flat background, these errors are of magnitudes about 10% of the perturbation peak value.

For *State* 3 with large numerical values of the anomalous second moments, we find a reasonable reconstruction at $t = 0$ of the normal second moments, but reconstruction of the anomalous second moments completely fails, unless we additionally include the observable $\hat{a}_0\hat{a}_0 + \hat{a}_0^\dagger\hat{a}_0^\dagger$ in the MAXENT density operator, as we did in section V B.

A squeezed condensate may be useful in atom interferometry as input to the dark side of an atomic mirror, whereupon a bright coherent input will be split with number fluctuations below the values for a binomial distribution [18]. It is in a similar setup that $\langle\hat{a}_0\hat{a}_0 + \hat{a}_0^\dagger\hat{a}_0^\dagger\rangle$ can be determined experimentally.

It is also worthy of notice that there was almost no improvement in the reconstruction from including additional position and momentum distributions for more points of time, and that using also the observable $\langle\hat{a}_0\hat{a}_0 + \hat{a}_0^\dagger\hat{a}_0^\dagger\rangle$ for *State* 1 and 2 did not change the precision of the reconstructed second moments.

As for states significantly different from the ones treated here, distributions in coordinate space at more points of time may be required for a reliable reconstruction. Since enlarging the number of measured distributions in space is rarely a problem, we suggest for specific application to gradually include more distributions until the results have stabilized. The calculation time is quite manageable, the shown examples all taking well under an hour on an ordinary PC.

VII. CONCLUSION

We have shown how to combine the MAXENT principle with the Bogoliubov approximation to give reliable estimates of the normal and anomalous second moments of the ladder operators, e.g. $\langle\hat{\psi}^\dagger(x)\hat{\psi}(x')\rangle$ and $\langle\hat{\psi}(x)\hat{\psi}(x')\rangle$, in a perturbed condensate. For states describable by a simple Gross-Pitaevskii equation, we find near perfect reconstruction from data of density distributions at a few points of time and the number of particles in the zero wave number mode. For states with a larger amount of particles in non-zero wave number modes compared to the size of the perturbation in coordinate space, we find it necessary to include a momentum distribution to obtain a somewhat reliable reconstruction. Errors in this case are less than 10% of the perturbation peak value (peak above the constant condensate background). Thus, the method makes it possible to distinguish between a thermal and a coherent perturbation of the condensate. Finally, we find that by measurement of a single observable related to squeezing, apart from measurements of momentum and coordinate space distributions, the method is able to correctly reconstruct all second moments of the ladder operators for squeezed states.

Appendix A: COMPUTATIONAL DETAILS

Several numerical problems may arise in finding the set $\{\lambda_\nu\}$ that satisfies Eqs. (1). As already touched upon towards the end of section II B, we have treated the problem as a minimization of deviations. We have chosen to minimize the vector of deviations Eq. (6) by using the Levenberg-Marquardt algorithm in the Matlab package. The most common problem encountered when using this approach is that for a given trial set $\{\lambda_\nu\}$, the matrix $\mathscr{P}$ in equation Eq. (45) may not be positive definite. This problem can be remedied somewhat by testing for positiveness using a Cholesky factorization, which takes negligible time compared with the para-unitary diagonalization. A better solution is to make a good initial guess to the values of $\{\lambda_\nu\}$. One can do this by first running the minimization with an almost uniform momentum distribution (in case this is included as observables) or with $\langle\hat{a}_0^\dagger\hat{a}_0\rangle$ set equal to N_{tot}/N, and then carrying out the subsequent program runs using the previously obtained $\{\lambda_\nu\}$ as initial values. In the subsequent program runs, one then gradually lets the momentum distributions approach the real distribution. A similar approach may be taken with the total number of particles, as making good guesses of the $\{\lambda_\nu\}$ may be easier at low particle numbers.

A trick we have made use of, which made guessing the $\{\lambda_\nu\}$ easier, is scaling down of the measured data. Since we are not interested in the true many-body density operator for the system, but only the second moments of the ladder operators, we may as well make the calculations for a smaller number of particles, provided the calculations are still precise, and then rescale the data afterwards. As an example, we shall show how to perform this down scaling in the b-basis at $t = 0$.

Let $\langle\boldsymbol{bb}^\dagger\rangle$ be the matrix of (unknown) second moments we wish to reconstruct. We will instead perform calculations on the matrix $\langle\boldsymbol{bb}^\dagger\rangle_{DS}$, also having the characteristics of a matrix of second moments:

$$\langle\boldsymbol{bb}^\dagger\rangle_{DS} = \kappa\left(\langle\boldsymbol{bb}^\dagger\rangle - \begin{pmatrix} I_N & 0 \\ 0 & 0 \end{pmatrix}\right) + \begin{pmatrix} I_N & 0 \\ 0 & 0 \end{pmatrix}$$

$$= \kappa\langle\boldsymbol{bb}^\dagger\rangle + (1-\kappa)\begin{pmatrix} I_N & 0 \\ 0 & 0 \end{pmatrix} \quad \text{(A1)}$$

where I_N is the $N \times N$ identity matrix and κ is a real number. When reconstructing the matrix $\langle \boldsymbol{b}\boldsymbol{b}^\dagger \rangle_{DS}$ we must modify the measurements, retaining gN_{tot} and thereby the transformation matrices $\mathscr{A}, \mathscr{B}$ and $\mathscr{U}$. So, for instance, the down scaled spatial density distributions that should be used can be found from:

$$
\langle \boldsymbol{\psi}(t)\boldsymbol{\psi}^\dagger(t) \rangle_{DS} = \kappa \langle \boldsymbol{\psi}(t)\boldsymbol{\psi}^\dagger(t) \rangle + (1-\kappa) \cdot
$$
$$
\mathscr{A}^{-1}\mathscr{B}^{-1} \begin{pmatrix} I_N & 0 \\ 0 & 0 \end{pmatrix} \left(\mathscr{A}^{-1}\mathscr{B}^{-1} \right)^\dagger .
$$

Comparing the lower half part of the diagonals, we see that we should multiply the coordinate space density measurements by κ and add to them $\frac{(1-\kappa)}{N} \sum_q v_q^2$. In a similar manner, measurements of other observables should be modified in the scaled down calculations. After the λ_ν has been found, the relation Eq. (A1) can easily be inverted, using the same point of time and basis as used in the original scaling.

Appendix B: WIGNER FUNCTIONS

It is common practise to map the $N \times N$ one-body density matrix to the real Wigner function $W(n,q)$ given on an $N \times N$ grid [19].

$$
W(n,q) = \frac{1}{N} \sum_{y=-M}^{M} \rho\left(f(n-y), f(n+y) \right) \cdot
$$
$$
\exp\left(4\pi i y n / N \right) \qquad \text{(B1)}
$$

$$
f(n-y) = \mod (n-y, N) - M - 1.
$$

The two arguments n and q can both assume N values, in our case $\{-M, -M+1, \ldots, M\}$, like in Eq. (12). The mapping is bijective so the Wigner function contains all the information in the one-body density matrix. Furthermore, the wave number- and spatial densities are easily recoverable:

$$
\langle \hat{\psi}^\dagger(x_n)\hat{\psi}(x_n) \rangle = \sum_{q=-M}^{M} W(n,q)
$$
$$
\langle \hat{a}^\dagger(k_q)\hat{a}(k_q) \rangle = \sum_{n=-M}^{M} W(n,q).
$$

In the case of only one particle, the evolution of the quantum system is completely described by the Hamiltonian and the one-body density matrix. In our case, having many particles, we instead have to specify all second moments to know the evolution of these, see Eq. (52). Therefore, in this paper, the Wigner function is merely meant as an illustration of the one-body density matrix at a particular point of time.

[1] E. A. Cornell and C. E. Wieman, *Nobel Lecture: Bose-Einstein condensation in a dilute gas, the first 70 years and some recent experiments*, Rev. Mod. Phys. **74**, p. 875-893 (2002)

[2] W. Ketterle, *Nobel lecture: When atoms behave as waves: Bose-Einstein condensation and the atom laser*, Rev. Mod. Phys. **74**, p. 1131-1151 (2002)

[3] E. T. Jaynes, *Information Theory and Statistical Mechanics II*, Phys. Rev. **108**, 2, p. 171-190, (1957)

[4] V. Bužek and G. Drobný, *Quantum tomography via the MaxEnt principle*, (Journal of Modern Optics) **47** no. 14/15, p. 28232839 (2000)

[5] G. Drobný and V. Bužek, *Reconstruction of motional states of neutral atoms via **MaxEnt** principle*, arXiv: quant-ph/0202080 v1. (2002)

[6] E. Skovsen, H. Stapelfeldt, S. Juhl, K. Mølmer, *Quantum state tomography of dissociating molecules*, Phys. Rev. Lett. **91**, 9, 090406/1-4 (2003)

[7] K. Vogel and H. Risken, *Determination of quasiprobability distributions in terms of probability distributions for the rotated quadrature phase*, Phys. Rev. A **40**, p. 2847-2849 (1989)

[8] J. Bertrand and P. Bertrand, *A tomographic approach to Wigner's function*, Found. Phys. **17**, p.397-405 (1987)

[9] G. M. D´Ariano, C. Macchiavello and M. G. A. Paris, *Detection of the density matrix through optical homodyne tomography without filtered back projection*, Phys. Rev. A **50**, p. 4298-4303 (1994)

[10] M. Olshanii, *Atomic Scattering in the Presence of an External Confinement and a Gas of Impenetrable Bosons*, Phys. Rev. Lett. **81**, p. 938-941 (1998)

[11] G. E. Astrakharchik, D. Blume, S. Giorgini and B. E. Granger, *Quasi-One-Dimensional Bose Gases with a Large Scattering Length*, Phys. Rev. Lett. **92**, 030402/1-4 (2004)

[12] N. Bogoliubov, *On the theory of superfluidity*, J.Phys. (USSR) **Vol. XI**, 1, p. 23-32 (1947), also reprinted in D. Pines, *The Many-Body Problem*, W.A. Benjamin Inc., New York 1961, p.292

[13] J. H. P. Colpa, *Diagonalizaton of the Quadratic Boson Hamiltonian*, Physica **93A** p.327-353 (1978)

[14] L. P. Pitaevskii and S. Stringari, *Bose-Einstein Condensation (International Series of Monographs on Physics)*, Clarendon Press, (2003)

[15] M. R. Andrews, M. O. Mewes, N. J. van Druten, D. S. Durfee, D. M. Kurn, and W. Ketterle, *Direct, Nondestructive Observation of a Bose Condensate*, Science **273**, p. 84-87, (1996)

[16] D. Leibfried, D. M. Meekhof, B. E. King, C. Monroe, W. M. Itano, and D. J. Wineland, *Experimental Determination of the Motional Quantum State of a Trapped Atom*, Phys. Rev. Lett. **77**, p. 4281-4285 (1996)

[17] A. I. Lvovsky, H. Hansen, T. Aichele, O. Benson, J. Mlynek, and S. Schiller, *Quantum State Reconstruction of the Single-Photon Fock State*, Phys. Rev. Lett. **87**, 050402/1-4 (2001)

[18] U. V. Poulsen and K. Mølmer, *Quantum states of Bose-Einstein condensates formed by molecular dissociation* , Phys. Rev. A **63**, 023604/1-11 (2001)

[19] U. Leonhardt, *Discrete Wigner functions and quantum state tomography*, Phys. Rev. A **50**, p. 2998-3013 (1996)

[20] The statement of the MAXENT procedure in this paper is very similar to the one given in f.x. [5]

[21] Going directly from Eq. (7), we have subtracted a constant, having no physical significance

[22] To follow [13] we use the, in matrix algebra unusual, prefix "para-" instead of f.x. "pseudo-".

[23] Had we been treating fermion- instead of boson-operators, the matrix $\mathcal{T}$ would have been unitary.

[24] An bilinear, hermitian operator can always be brought to this form by adding a scalar constant which is determined by the diagonal of the matrix.